ELSEVIER

Thermochimica Acta 318 (1998) 91–100

thermochimica acta

Kinetics and mechanism of thermal oxidation of sialon ceramic powders

Kenneth J.D. MacKenzie[a,*], Carolyn M. Sheppard[a], Glen C. Barris[a], Ann M. Mills[a], Shiro Shimada[b], Hajime Kiyono[b]

[a] *New Zealand Institute for Industrial Research and Development, P.O. Box 31-310, Lower Hutt, New Zealand*
[b] *Faculty of Engineering, Hokkaido University, Sapporo, Japan*

Received 9 September 1997; accepted 30 November 1997

Abstract

X-ray diffraction, solid state MAS NMR and isothermal thermogravimetry were used to study the oxidation mechanism and kinetics of pure X-phase and O′-sialon powders prepared by silicothermal synthesis. X-phase sialon ($Si_{12}Al_{18}O_{39}N_8$) begins to oxidise at above 940°C, forming amorphous silica and progressively losing nitrogen from the SiO_2N_2 groups to form mullite at 1200–1300°C. O′-sialon is more oxidation-resistant; although significant formation of amorphous silica occurs above 940°C, the crystalline products (silica and a small amount of mullite) appear above 1235°C. At 1400–1600°C, oxidation is progressively hindered by the formation of a protective fused silica surface layer containing octahedral Al. The oxidation kinetics can be described by a parabolic rate law, with temperature coefficients of reaction rate (E_a) of 250 and 454 kJ mol^{-1} for X-phase and O′-sialon, respectively. The kinetic results are discussed in the context of previous sialon powder oxidation studies. © 1998 Elsevier Science B.V.

1. Introduction

Sialons are compounds of silicon, aluminium, oxygen and nitrogen which have found applications as engineering ceramics, cutting tools and refractory materials. They occur in a range of compositions (Fig. 1) with structures closely related to those of the oxide or nitride parent material from which they are derived by substitution of Al for Si and O for N. Fig. 1 indicates the compositional relationships between three of the best known sialon phases falling within the SiO_2–Si_3N_4–AlN–Al_2O_3 diagram of state (β′-sialon, O′-sialon and X-phase sialon). β′-sialon is structurally related to β-Si_3N_4 and has the composition $Si_{6-z}Al_zO_zN_{8-z}$ where z ranges from 0 (corresponding to pure Si_3N_4) to ca. 4.3. O′-sialon may be considered as Al-substituted Silcon oxynitride, with the formula $Si_{2-x}Al_xO_{1+x}N_{2-x}$ where x ranges from 0 (pure Si_2N_2O) to ca. 0.4 at 1900°C. The structure of X-phase sialon, $Si_{12}Al_{18}O_{39}N_8$, is similar to mullite ($Al_6Si_2O_{13}$) and exists over a narrow solid solution range between Si_3N_4 and mullite.

An important practical restriction on the use of all these oxynitrides at elevated temperatures in air is their tendency to oxidise, although in practice, such thermal degradation may be slow in highly dense bodies with limited internal access of air [1], and may also be influenced by the presence of dopants added to assist the densification process [2]. Undoped sialon powders represent the most favourable situation for oxidation, but by contrast with Si_3N_4 which has been extensively investigated (see references in [3]), kinetic and mechanistic information on the oxidation processes in these materials is limited to a recent study

*Corresponding author.

PII S0040-6031(98)00333-5

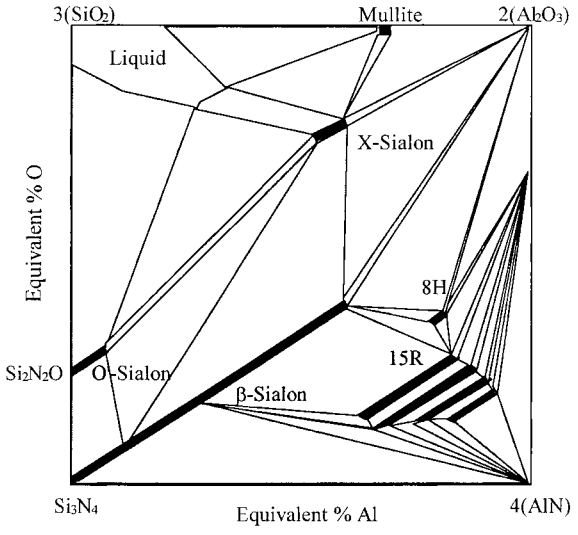

Fig. 1. Diagram of state for the sialon system at 1700–1730°C, adapted from Ref. [18].

of β′-sialon (z=2.45) powder prepared by carbothermal synthesis [3]. In that study, the evolution of the oxidation products (mullite and silica) was monitored by X-ray diffraction of the crystalline phases and by solid-state nuclear magnetic resonance spectroscopy (MAS NMR) to determine the behaviour of the X-ray amorphous material [3]. The oxidation kinetics, determined by isothermal thermogravimetry, could be described satisfactorily at 1100–1300°C by a parabolic rate law with an activation enthalpy of 161 kJ mol^{-1}, suggesting that the rate is controlled by the permeation of oxygen through the product layer developing on the grains [3].

The purpose of the present work is to extend these powder oxidation studies to the two other important sialon phases, namely X-phase sialon and O′-sialon, which we have synthesised in a pure form by a silicothermal method. The results are compared with those previously determined for β′-sialon [3].

2. Experimental

The X-phase sialon was synthesised by silicothermal reaction of kaolinite (BDH 'light'), silicon powder (Permascand 4D) and γ-Al_2O_3, prepared by heating $Al(OH)_3$ (BDH reagent grade) at 800°C for 3.5 h. These components were mixed to give the composition $Si_{12}Al_{18}O_{39}N_8$ and ball milled under hexane for 20 h using silicon nitride milling media. After removal of the solvent by vacuum rotary evaporator, the solid material was pressed into 25 mm diameter discs and fired at 1500°C for 4 h under flowing purified nitrogen. XRD of the powdered product showed it to be monophase X-phase sialon, with a very small trace of mullite impurity. Reported compositions of X-phase sialon vary from $SiAlO_2N$ to $Si_{16.9}Al_{22.7}O_{48.8}N_{11.6}$ [6], and the true composition of the present phase may vary from the target composition if either under-reaction or over-reaction has occurred; previous studies [6] have indicated the presence of mullite and/or free alumina in silicothermal product assemblages. The XRD pattern does not provide an accurate indication of composition, since all the published patterns for a variety of reported stoichiometries have the major peaks in common, with small variations probably due to the presence of impurity phases such as O′-sialon [6].

The O′-sialon was prepared by blending together the above kaolinite, Si powder and powdered SiO_2 (Commercial Minerals superfine quartz) to produce the composition $Si_9AlO_6N_9$ (O′-sialon, x=0.2). Before use in O′-sialon synthesis, the kaolinite was dehydroxylated at 800°C for 1 h. After ball milling as for X-phase sialon, the solid material was lightly extruded into rods then fired at 1450°C for 8 h under flowing purified nitrogen (30 ml min^{-1}). The product contained a proportion of X-ray amorphous material which was crystallised by heat treatment of lightly pressed pellets at 1720°C for 2 h in flowing purified nitrogen. The powdered product was essentially monophase O′-sialon of composition x=0.18, determined by careful measurements of the unit cell parameters by powder XRD (Philips PW 1700 computer-controlled diffractometer with CoK_α radiation and graphite monochromator). A small amount of β-Si_3N_4 impurity was also detected by XRD; its concentration was determined by a quantitative Rietveld powder XRD procedure [4] to be 7.7%. Using alumina as an internal standard, the Rietveld analysis also determined the presence of 0.4% X-phase impurity and 2.7% amorphous phase.

The particle size distribution of the O′-sialon determined by laser interferometer (Shimadzu Sald-2001) was: 100%<30, 50%<3 and 10%<0.7 μm. The corre-

sponding particle size distribution of the X-phase sialon was: 100%<50, 50%<5 and 10%<1 μm.

Samples of the sialons were oxidised in platinum crucibles in an electric muffle furnace for 1 h at temperatures between 940 and 1600°C then examined by XRD and MAS NMR at 11.7 T (Varian Unity 500 spectrometer with a 5 mm Doty probe spun at 9–12 kHz) under the following conditions:

^{29}Si; 6 μs $\pi/2$ pulse, recycle delay 100 s, shifts referenced to tetramethylsilane (TMS);
^{27}Al; 1 μs $\pi/10$ pulse for solution, recycle delay 5 s, shifts referenced to 1 M aqueous $Al(NO_3)_3$ solution.

The oxidation kinetics were measured by isothermal thermogravimetry at 1000–1400°C using a Cahn Model 2000 thermobalance and a Rheometrics STA 1500 thermoanalyser. The samples (10–50 mg) were brought to the reaction temperature at 20°C min under a flowing atmosphere of nitrogen or ultra high purity argon (99.9995%) and equilibrated before changing to the oxidising atmosphere (flowing air at 50 ml min or 80 : 20 Ar/O_2 mixture at 100 ml min) and monitoring the mass change continuously for 2–4 h. The gas inlet is located in the immediate region of the sample, ensuring that the introduction of oxygen will have a rapid effect on the sample; nevertheless, a finite time, possibly a few minutes, may elapse before the undiluted oxidising atmosphere is fully established in the thermobalance. The reactivity of the present powders was such that the oxidation times used here were sufficient to establish the reaction kinetics.

The surface areas of the powders before and after oxidation were measured using a Quantasorb nitrogen absorption apparatus.

3. Results and discussion

3.1. Oxidation reactions in X-phase sialon

Fig. 2 summarises the XRD data for X-phase powder samples oxidised at various temperatures for 1 h. The reported XRD intensities for each detected crystalline phase refer to the X-phase sialon 320 reflection at d=3.611 Å, the 110 mullite reflection at d=5.39 Å and the 101 cristobalite reflection at d=4.05 Å; where non-major reflections are used, the intensities have been scaled to that of the major reflection using the PDF-listed intensity ratios. The XRD intensity of X-phase sialon has begun to decrease even at 940°C, and continues to do so with increasing temperature, but without corresponding formation of crystalline products until the appearance of mullite in the sample oxidised at 1235°C and a small amount of cristobalite (SiO_2) at 1430°C (Fig. 2).

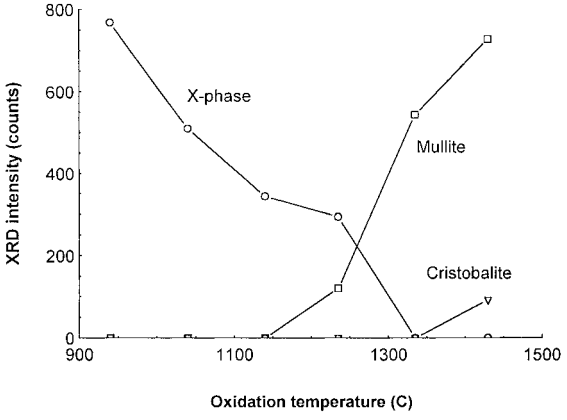

Fig. 2. Semi-quantitative representation of the crystalline phases in oxidised X-phase sialon powder as a function of the oxidation temperature.

The lattice parameters of the crystalline mullite product, determined using silicon as the angular calibrant, yield via the relationship of Cameron [5] mullite compositions of 61 and 59 mol% Al_2O_3 at 1335 and 1430°C, respectively, i.e. the oxidation product is 3 : 2 mullite ($Al_6Si_2O_{13}$).

The ^{29}Si MAS NMR spectra of the unoxidised and oxidised X-phase samples are shown in Fig. 3.

The unoxidised spectrum (Fig. 3(A)) is similar to that previously published for X-phase produced by silicothermal reaction [6], but contains an additional broad feature at −108 ppm corresponding to uncombined X-ray amorphous SiO_2. Integration of this spectrum indicates the amount of additional Si is ≈25% of the total ^{29}Si signal, corresponding to an additional 3 mol SiO_2 per mole of X-phase. Oxidation at 940°C significantly increases the amount of uncombined SiO_2 (Fig. 3(B)), also broadening and shifting the feature at ca. −77 (attributed to SiO_3N groups [6]) towards the characteristic tetrahedral Si–O frequency of mullite (−86 ppm [7]). At this early stage of oxidation, the two features at −55 and −66 ppm also

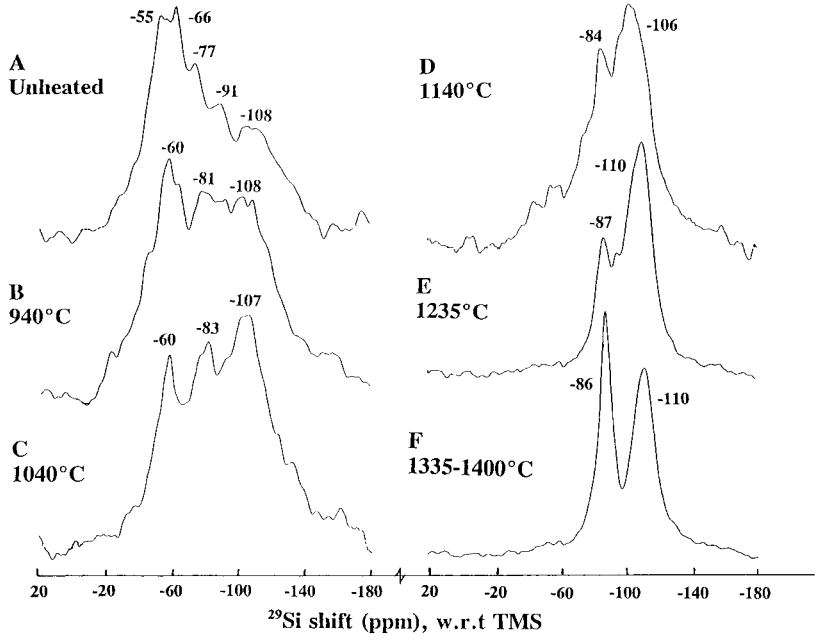

Fig. 3. Representative 11.7 T ^{29}Si MAS NMR spectra of X-phase sialon powder oxidised for 1 h at the indicated temperatures.

merge, suggesting the conversion of SiO_2N_2 groups to SiO_3N; the loss of nitrogen from the structure therefore sets in early, with the formation of amorphous SiO_2 and mullite-like regions which are however too small or too disordered to be detected by XRD. At 1040°C, the concentration of SiO_2 and mullite-like structures has increased but the persistence of the −60 ppm resonance suggests that significant numbers of SiO_3N units remain (Fig. 3(C)); these disappear rapidly at 1140°C (Fig. 3(D)) although the structure retains the XRD characteristics of X-phase sialon rather than mullite which begins to appear at 1235°C (Fig. 2). At 1335–1430°C, the ^{29}Si spectra (Fig. 3(F)) are typically those of mullite (−86 ppm) and SiO_2 (−110 ppm). The changes in the Si distribution over the various phases, estimated by spectral integration, are shown in Fig. 4.

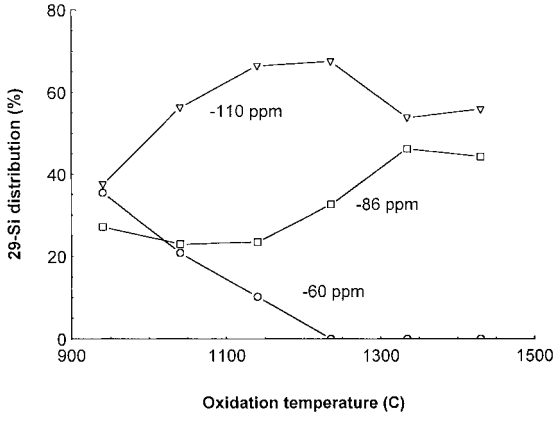

Fig. 4. Partitioning of ^{29}Si over the various sites in oxidised X-phase sialon powder as a function of the oxidation temperature.

Since the products of complete oxidation of X-phase sialon are mullite and SiO_2, the oxidation equation may be written

$$Si_{12}Al_{18}O_{39}N_8 + 6O_2 \rightarrow 3Al_6Si_2O_{13} + 6SiO_2 + 4N_2 \uparrow \quad (1)$$

Eq. (1) predicts a mass gain of 5.1% and a ratio of Si in mullite to Si in SiO_2 of 1.0 in the fully oxidised material. The observed Si ratios at 1335 and 1430°C are 0.86 and 0.79, respectively, consistent with the presence of ca. 12.5% Si as additional SiO_2. Since the unoxidised sample contained ≈25% additional Si, about half of this has been lost by 1335°C, possibly during equilibration or in the early stages of oxidation, when the SiO_2 present may

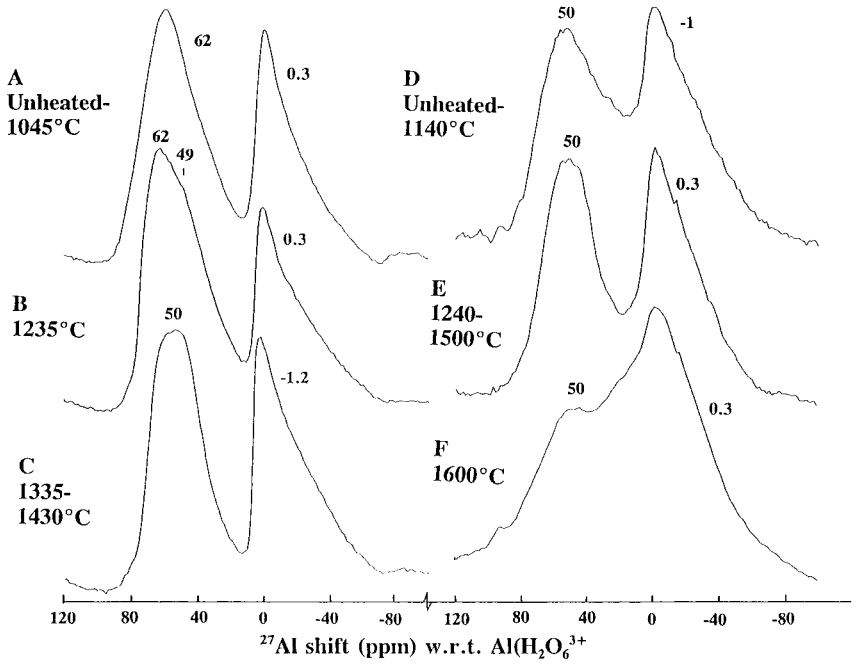

Fig. 5. Representative 11.7 T ^{27}Al MAS NMR spectra of sialon powders oxidised for 1 h at the indicated temperatures. A–C, X-phase sialon. D–F, O′-sialon.

decompose to SiO under conditions of low oxygen partial pressure.

Typical ^{27}Al MAS NMR spectra of oxidised and unoxidised X-phase sialons are shown in Fig. 5(A–C), which shows in all the spectra the presence of tetrahedral and octahedral Al–O units at 50–60 ppm and ca. 0 ppm, respectively.

While the position of the octahedral Al resonance remains at 0.3 ppm up to 1335°C, the tetrahedral Al shift is more sensitive to the oxidation reactions (Fig. 6), moving progressively from the typical X-phase value of ca. 62 ppm [6] towards 49.9 ppm at 1430°C; the latter value represents the mean of the two tetrahedral shifts of pure crystalline mullite [7] which are unresolved in the present spectra. These changes in tetrahedral position are accompanied by a change in the relative amount of tetrahedral Al, estimated by integrating the ^{27}Al spectra (Fig. 7), which show between 1200°C and 1300°C an abrupt change from typical X-phase values to the value for well-crystallized mullite at 11.7 T (52% [7]). These spectra show no indication of the free alumina noted in a previous

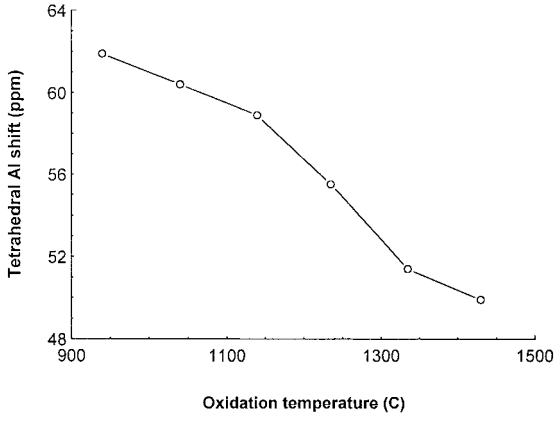

Fig. 6. Tetrahedral ^{27}Al chemical shift of X-phase sialon powder as a function of oxidation temperature.

study at ca. 13 ppm [6], but the broadness of the present resonances may mask such a feature.

In summary, the oxidation of X-phase sialon begins below 940°C with the formation of amorphous SiO_2 and the loss of nitrogen from tetrahedral SiO_2N_2

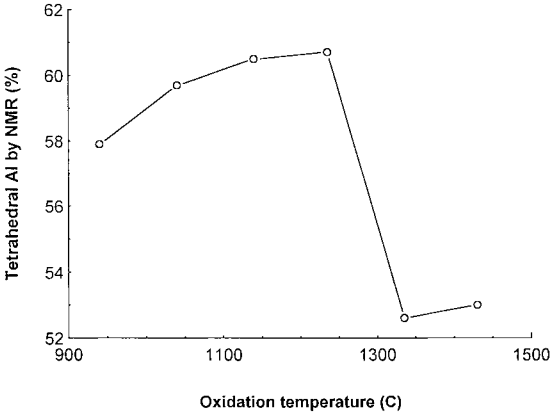

Fig. 7. Percentage of tetrahedral ^{27}Al in X-phase sialon powder as a function of oxidation temperature.

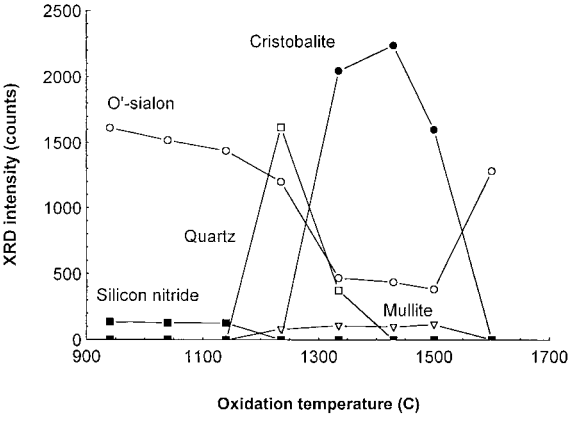

Fig. 8. Semi-quantitative representation of the crystalline phases present in oxidised O′-sialon powder as a function of the oxidation temperature.

structural groups which progress via SiO_3N towards the tetrahedral Si–O groups of mullite, taking on typical XRD and ^{27}Al NMR characteristics between 1200 and 1300°C. At higher temperatures, some of the amorphous SiO_2 transforms to cristobalite, but NMR estimates of Si partitioning amongst the phases suggest that some SiO_2 is also lost from the system through the vapour phase.

3.2. Oxidation reactions in O′-sialon

Fig. 8 shows the oxidation behaviour of O′-sialon powder, monitored by XRD using the 200 reflection of O′-sialon at d=4.449 Å, the 200 reflection of β-Si_3N_4 at d=3.293 Å, the 101 reflection of cristobalite at d=4.05 Å, the 100 peak of quartz at d=4.26 Å and the 110 peak of mullite at d=5.39 Å, all scaled to the major intensity for each phase.

The XRD data suggest that the O′-sialon powder is more resistant to oxidation than X-phase sialon, displaying a significant intensity loss only above 1235°C, accompanied by the transitory appearance of SiO_2 (quartz) and a small amount of mullite (Fig. 8). The phase labelled quartz has an a-parameter slightly expanded to ≈4.94 Å, suggesting a stuffed structure; an expanded a-parameter is also found in the cristobalite which replaces this quartz at higher temperatures. Measurements of the a-dimension of the O′-sialon during oxidation indicate that the composition parameter x maintains a mean value of 0.21 over the temperature range from 20 to 1600°C. By contrast with the behaviour of X-phase sialon, the O′-sialon reflections do not completely disappear above 1335°C, and are strongly present as the sole crystalline phase at 1600°C, together with evidence of considerable amorphous material. This unexpected high-temperature behaviour appears to be associated with fusion and sintering of the powder which is seen by SEM to contain highly siliceous glassy fragments; these seem to protect the underlying sialon from further oxidation.

Fig. 9 shows a selection of ^{29}Si MAS NMR spectra of unoxidised and oxidised O′-sialon powders.

The ^{29}Si spectrum of the unheated material (Fig. 9(A)) shows, in addition to the O′-sialon resonance at −60.3 ppm and the Si_3N_4 impurity at −47.4 ppm, a broad resonance at ca. −110 ppm corresponding to an additional impurity phase (X-ray-amorphous SiO_2). Oxidation at 940°C significantly increases the amorphous SiO_2 peak by comparison with the O′-sialon and Si_3N_4 resonances, which begin to decrease at ca. 1100°C (Fig. 9(D)) and have virtually disappeared at ca. 1235°C (Fig. 9(E)). Above ca. 1300°C, oxidation becomes slower and less complete, as evidenced by the persistence of the sialon resonance (Fig. 9(F)); at 1600°C the sialon peak at −60.2 ppm is prominent (Fig. 9(G)), but the increased broadness of the SiO_2 resonance suggests that this phase has melted, protecting the sialon from further oxidation. Evidence of mullite development is obscured at the lower temperatures by the overlap

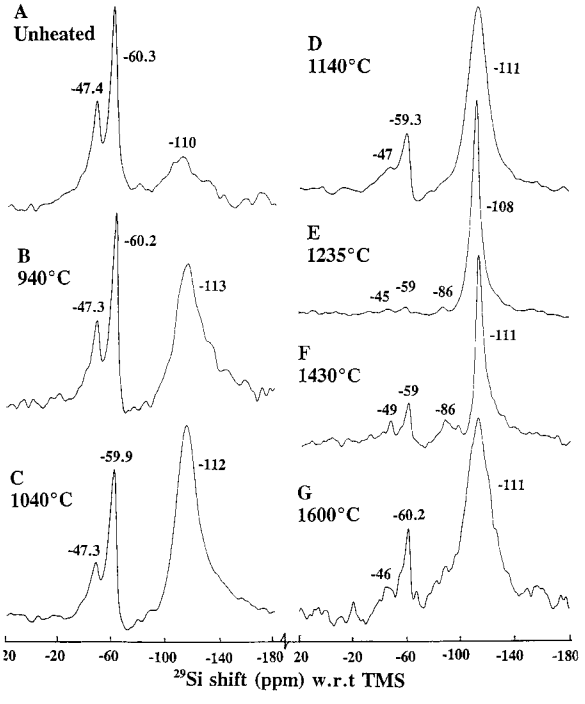

Fig. 9. Representative 11.7 T ^{29}Si MAS NMR spectra of O′-sialon powder oxidised for 1 h at the indicated temperatures.

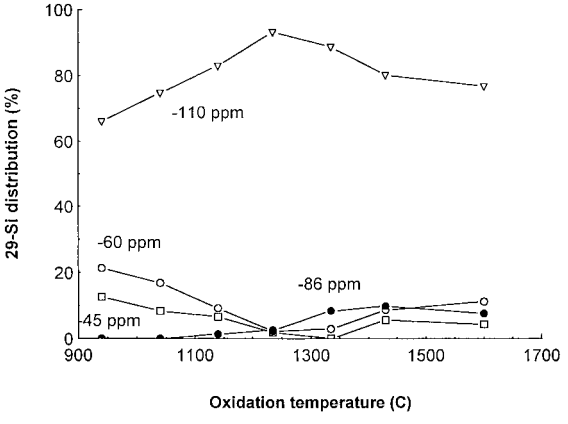

Fig. 10. Partitioning of ^{29}Si over the various sites in oxidised O′-sialon powder as a function of the oxidation temperature.

of the broad silica envelope into the characteristic mullite region (−86 to −94 ppm); at ca. 1200–1500°C the presence of a small amount of mullite can be seen more clearly alongside the narrowed cristobalite peak (Fig. 9(E,F)). The changes in the distribution of the Si over the various Si-containing phases during oxidation, derived by integration of the ^{29}Si spectra, are shown in Fig. 10.

Typical ^{27}Al spectra of the unoxidised and oxidised O′-sialons are shown in Fig. 5(D–F). These indicate that the small amount of Al present occupies both tetrahedral and octahedral sites in the unoxidised sample and throughout oxidation, but at 1600°C the resonances have become broadened and overlapping (Fig. 5(F)). The ratio of tetrahedral to octahedral Al, estimated by spectral integration, remains in the range of 3 : 2 mullite (48.7–52.5%) below 1600°C, at which temperature it drops to 29.2%. Although the structure of unoxidised O′-sialon contains only tetrahedral Al, the octahedral Al which is always additionally present has been attributed to secondary impurity phases [8]; if this is the case, the occurrence of a mullite-like tetrahedral/octahedral ratio in the present unoxidised sample and the samples oxidised below 1240°C may represent a fortuitous combination of overlapping tetrahedral intensities. Between 1240 and 1500°C the tetrahedral envelope becomes more mullite-like (cf. Fig. 5(C)) and probably reflects the presence of mullite, as also indicated by XRD. The increased and broadened octahedral intensity at 1600°C confirms the incorporation of some Al into a Si-rich amorphous fusion product.

In summary, O′-sialon appears by XRD to be stable to oxidation below 1235°C; ^{29}Si NMR reveals however the formation of significant amounts of X-ray amorphous SiO_2 as low as 940°C. Above ca. 1235°C, crystallization of the oxidation products (SiO_2 and a small amount of mullite) occurs, but in samples heated directly to 1430–1600°C in air, oxidation is progressively hindered with increasing temperature, possibly by the formation of a protective fused surface layer. Samples quenched from 1600°C contained no crystalline oxidation products, but the occurrence of an expectedly high proportion of Al in octahedral sites suggests its partial incorporation into the X-ray amorphous silica-rich fused material.

3.3. Oxidation kinetics of X-phase sialon

Isothermal mass gain curves as a function of time for a series of oxidation temperatures are shown in Fig. 11(A), in which the surface area of all the samples, measured by nitrogen adsorption at the

conclusion of the oxidation at 900–1100°C, was 3.3 $m^2 g^{-1}$.

Irregularities in the kinetic curves during the first few minutes of the reaction, which were most noticeable at 900–1000°C, may result from delays in establishing a strongly oxidising atmosphere around the sample.

The oxidation kinetics of other sialon and silicon nitride powders have previously been described [3] by a parabolic rate law:

$$(\Delta W/A)^2 = kt + c \quad (2)$$

where ΔW is the oxidation mass change per unit area A, k the reaction rate constant and c a numerical constant. Other rate laws such as those of Carter [15] which take into account changes in the size of the unoxidised particle during reaction, and of Deal and Grove [16], which provide for an initial non-parabolic period could be more appropriate to the present system, but the parabolic rate law was used here in order to make direct comparisons with previously published results. Plots of $(\Delta W/A)^2$ vs. oxidation time (Fig. 12(A)) show reasonable linearity up to 60–120 min, but do not all pass through $t=0$, in consequence of the initiation period. The temperature coefficient of the oxidation rate (E_a), determined from the Arrhenius plot (Fig. 13(A)) is 250 kJ mol^{-1}, considerably greater than the E_a determined for β′-sialon powder with $z=2.45$ (161 kJ mol^{-1} [3]).

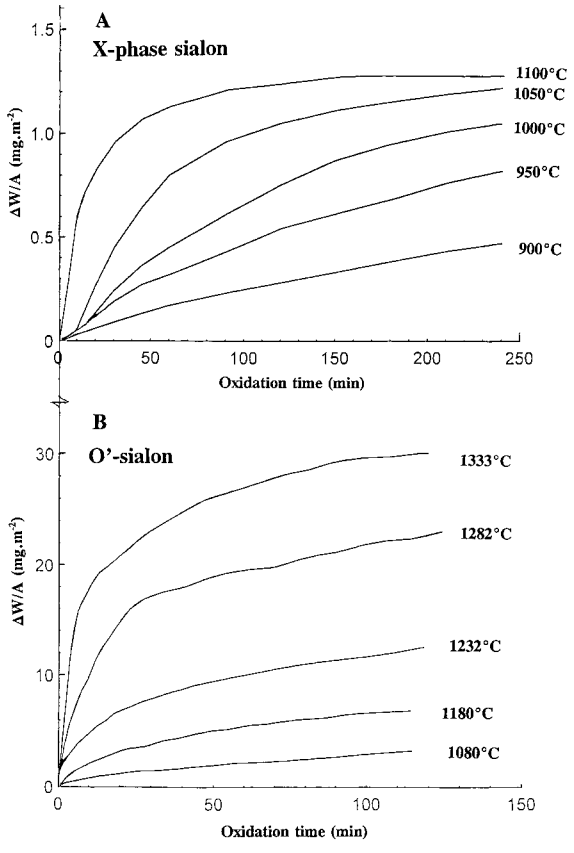

Fig. 11. Kinetic curves for the isothermal oxidation of A, X-phase sialon powder, B, O′-sialon powder.

3.4. Oxidation kinetics of O′-sialon

The isothermal mass gain curves for O′-sialon are shown in Fig. 11(B), plotted using the measured surface areas of these oxidised samples, which changed from 13.5 $m^2 g^{-1}$ at 900°C to 2.8 $m^2 g^{-1}$ at 1300°C. The upper temperature of these kinetic experiments was chosen so as to avoid the passivation effect of the glassy surface layer noted at higher temperatures. The kinetic curves also showed evidence of an initial slow period, particularly in the experiments conducted using the Cahn thermobalance (not shown in Fig. 11(B)). This effect did not however influence the subsequent kinetic analysis or lead to a different E_a value. For consistency with previous results [3], the kinetic curves were again fitted by a parabolic rate law, which satisfactorily describes the early stage of the reaction (Fig. 12(B)). The resulting E_a value (Fig. 13(B)) is 454 kJ mol^{-1}, reflecting the considerably greater oxidation resistance of this sialon.

3.5. Comparison with previous sialon oxidation studies

Although Eq. (2) fits the data for both sialons reasonably well over the complete temperature range, the indications of an initial induction period may not be due solely to experimental technique, but could also suggest the presence of an oxidised layer on the original particles, or genuine initial linear oxidation behaviour, or both. Similar initial behaviour has been reported in a study of the oxidation of Si_3N_4 powder [9], and also in a low-temperature oxidation study of carbothermal β′-sialon [10], in which the initial kinetics were fitted by a linear rate law which however

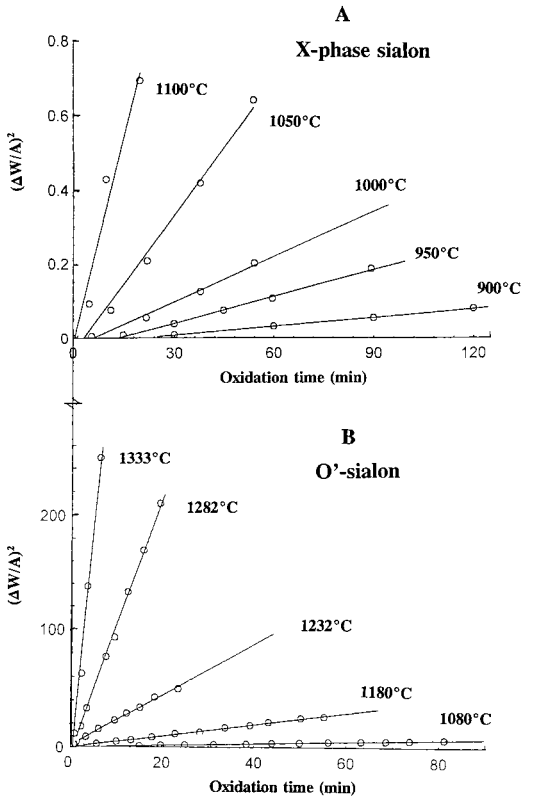

Fig. 12. Kinetic data plotted according to the parabolic rate law for the oxidation of A, X-phase sialon powder, B, O′-sialon powder.

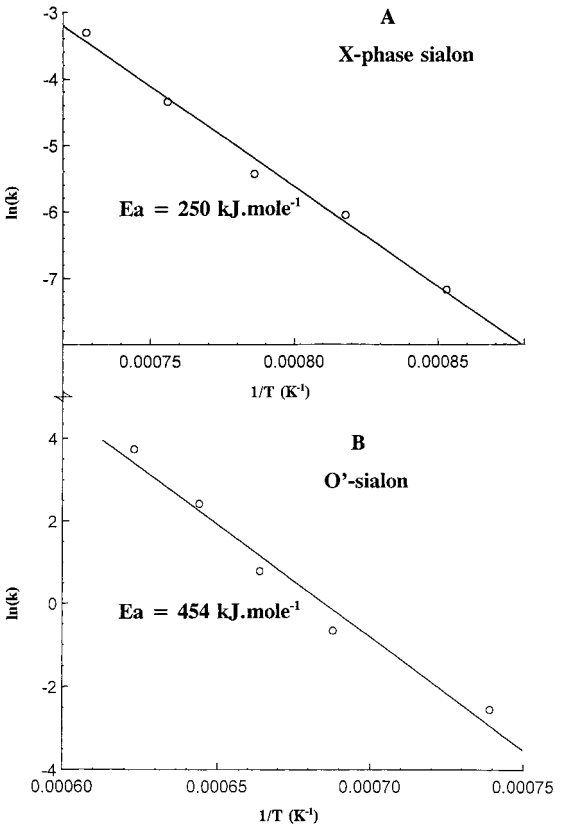

Fig. 13. Arrhenius plots for the oxidation of A, X-phase sialon powder, B, O′-sialon powder.

gave a similar E_a value (170 kJ mol^{-1}) to the parabolic kinetics followed over a wider temperature range by the same material (161 kJ mol^{-1}). The similarity between these values and the E_a for oxygen diffusion in SiO_2 and mullite has previously been noted [3,10]. Further studies are in progress to investigate in greater detail the initial oxidation stages of both X-phase and O′-sialon.

The E_a value for X-phase sialon is within the range of values reported for Si_3N_4 powders (147–285 kJ mol^{-1} [11,9]); here the diffusional rate-determining process corresponding to activation energies which are clearly much higher than for oxygen diffusion in SiO_2 has not been determined. The E_a value for O′-sialon oxidation is even larger, being more typical of densified pellets of β′-sialon [2] or Si_3N_4 [13], but larger than the E_a value reported [17] for the oxidation of hot isostatically pressed pellets of Si_2N_2O (245 kJ mol^{-1}). Two possible rate-limiting processes which have been suggested in connection with the oxidation of hot-pressed Si_3N_4 are the outward diffusion of nitrogen or the interdiffusion of cations introduced as sintering aids [12]). Although diffusion data for nitrogen in these systems are sparse, it has been suggested that the substitution of oxygen by nitrogen in the glassy oxidation product leads to a stiffer oxide network and a higher activation energy for oxygen transport [14]. On this basis, it might be expected that sialons containing the maximum nitrogen available for incorporation into the oxidation layer should be the most oxidation resistant, but this simple concept is not consistent with the nitrogen contents of the present three sialons (27.5, 7.2 and 18.3 mass% in β′, X-phase and O′-sialon, respectively).

The present E_a values for oxidation of X-phase and O′-sialon are comparable with those for cation diffusion in oxides and silicates, but since cationic sintering aids were not present in our sialons, the diffusing species is limited to Al^{3+}, which was shown by MAS NMR to be present in the glassy product associated with our oxidised O′-sialon. The incorporation of cations into the glassy phase is known to influence its viscosity, and has been implicated in the oxidation of hot-pressed compacts of β′-sialon [1], in which the resistance to oxidation was reported to increase with increasing Al content. However, this simple rule does not appear to hold for our present materials, in which the Al contents of the β′, X-phase and O′-sialon are 23.4, 31.2 and 5.9 mass%, respectively. The oxidation behaviour of these sialons therefore appears to be determined by a combination of factors which could include the composition and viscosity of the oxidation layer, but may also reflect the changes in atomic configuration needed to form mullite and silica from sialons of different structure.

Acknowledgements

We are indebted to K. Card for the SEM observations and to R.A. Fletcher for the surface area measurements.

References

[1] S.C. Singhal, F.F. Lange, J. Amer. Ceram. Soc. 60 (1977) 190.
[2] T. Chartier, J.L. Besson, P. Goursat, Int. J. High Tech Ceramics 2 (1986) 33.
[3] K.J.D. MacKenzie, S. Shimada, T. Aoki, J. Mater. Chem. 7 (1997) 527.
[4] SIROQUANT for Windows, Version 2.0 (1996), Sietronics Pty. Ltd., Australia.
[5] W.E. Cameron, Bull. Amer. Ceram. Soc. 56 (1977) 1003.
[6] C.M. Sheppard, K.J.D. MacKenzie, G.C. Barris, R.H. Meinhold, J. Eur. Ceram. Soc. 17 (1997) 667.
[7] L.H. Merwin, A. Sebald, H. Rager, H. Schneider, Phys. Chem. Minerals 18 (1991) 47.
[8] J. Sjöberg, R.K. Harris, D.C. Apperley, J. Mater. Chem. 2 (1992) 433.
[9] R.M. Horton, J. Amer. Ceram. Soc. 52 (1969) 121.
[10] S. Shimada, T. Aoki, H. Kiyono, K.J.D. MacKenzie, J. Amer. Ceram. Soc. 82 (1998) 266.
[11] P. Goursat, P. Lortholary, D. Tetard, M. Billy, Proc. Int. Symp. React. Solids, Bristol, 1972, in: J.S. Anderson (Ed.), Chapman and Hall, London, 1972, pp. 315–326.
[12] S.C. Singhal, J. Mater. Sci. 11 (1976) 500.
[13] D. Cubicciotti, K.H. Lau, J. Amer. Ceram. Soc. 61 (1978) 512.
[14] D.P. Butt, D. Albert, T.N. Taylor, J. Amer. Ceram. Soc. 79 (1996) 2809.
[15] R.E. Carter, J. Chem. Phys. 34 (1961) 2010.
[16] B.E. Deal, A.S. Grove, J. Appl. Phys. 36 (1965) 3770.
[17] J. Persson, P.-O. Käll, M. Nygren, J. Amer. Ceram. Soc. 75 (1992) 3377.
[18] B. Bergman, T.C. Ekström, A. Micski, J. Eur. Ceram Soc. 8 (1991) 141.